

GENERALIZED DOUBLE BRACKET VECTOR FIELDS

PETRE BIRTEA, ZOHREH RAVANPAK, AND CORNELIA VIZMAN

ABSTRACT. By introducing a metriplectic tensor, we generalize the double bracket vector fields defined on semi-simple Lie algebras to the case of Poisson manifolds endowed with a pseudo-Riemannian metric. We also construct a generalization of the normal metric on an adjoint orbit of a compact semi-simple Lie algebra such that the above vector fields, when restricted to a symplectic leaf, become gradient vector fields. We illustrate the newly introduced objects to a variety of examples and carefully discuss complications that arise when the pseudo-Riemannian metric does not induce a non-degenerate metric on parts of the symplectic leaves.

1. INTRODUCTION

On a Riemannian manifold, one of the questions is how can one compute the gradient vector field of a cost function. This problem appears, for instance, in designing steepest descent algorithms on Riemannian manifolds, like matrix Lie groups and homogeneous spaces. To answer this, one needs to have sufficient information on the metric in order to solve the equation that defines the gradient vector field. This is oftentimes not possible or leads to very tedious computations.

A more amenable case is when our manifold of interest is realized as a submanifold in an ambient Riemannian manifold with a simpler Riemannian geometry, so that one can explicitly construct the orthogonal projection operator that relates the gradient vector fields in the two manifolds. This approach has been extensively applied in constrained optimization problems, e.g. in [1][13].

In the often encountered case of a submanifold described by a set of constraint functions, the gradient vector field on the submanifold, with respect to the induced metric, can be realized as a restriction of a vector field (called embedded gradient vector field) defined on the ambient space. This construction has been worked out in [5][6].

Sometimes it happens that not enough components of the constraint map that defines the submanifold are available. This case appears, for instance, when one does not explicitly know enough Casimirs to describe a symplectic leaf of a Poisson manifold. Nevertheless, in the case of the Lie-Poisson structure for a compact Lie algebra, the gradient vector field on the regular symplectic leaves has been obtained as the restriction of a vector field on the ambient space, namely the double bracket vector field. Unlike in the previous setting, the metric on the symplectic leaf will not be the induced one, but the so called normal metric.

2020 *Mathematics Subject Classification.* 53D17, 58D17, 17B20.

Key words and phrases. Poisson manifold, Riemannian manifold, double bracket vector field, Lie Poisson structures, Poisson-Lie groups .

Our goal is to obtain an analogue of the above scenario in the setting of a general Poisson manifold equipped with a (pseudo-)Riemannian metric.

More precisely, following an idea presented in [5], we construct a symmetric contravariant tensor that couples the Poisson structure and the Riemannian structure (no compatibility conditions required). This type of tensors are called in the literature metriplectic tensors [16][17][20]. Our newly constructed tensor allows to associate a vector field to every smooth function in a naturally way. We call this vector field the generalized double bracket vector field as, for the case of a compact semi-simple Lie algebra, we recover the classical double bracket vector field. The generalized double bracket vector field has some useful properties. It is tangent to all the symplectic leaves. Moreover, when restricted to such a leaf, it proves to be of gradient type with respect to a natural metric that generalizes the normal metric.

All the constructions above work more generally for a pseudo-Riemannian structure on the Poisson manifold. Thus, non-compact semi-simple Lie algebras can be included. The trade off is that in this case one needs to restrict to what we will call good symplectic leaves, namely those for which the induced metric is non-degenerate.

However, new complications arise in the nonlinear Poisson setting. An important question is if the restriction of the indefinite signature metric to the symplectic leaves is non-degenerate. While for the special case of a non-compact semi-simple Lie algebra this happens on some exceptional leaves only, in the general case, the situation is more intricate and this question will occupy us for a good part of this paper. We will in particular look at the case of the Lie algebra $\mathfrak{sl}(2, \mathbb{R})$ and a huge class of Poisson structures on \mathbb{R}^3 generalizing it non-linearly, while keeping a rescaling of the Killing form of $\mathfrak{sl}(2, \mathbb{R})$ in the ambient space \mathbb{R}^3 . This will lead to an interesting and sophisticated interplay between the Poisson and the pseudo-Riemannian structures.

Our constructions that generalize the double bracket vector fields are suitable for the study of various dynamical properties of dissipative systems, analogous to other methods, e.g. those used in [7][18].

Structure of the paper. We start Section 2 by recalling the classical double bracket vector field in the linear case of a semi-simple Lie algebra \mathfrak{g} . In order to generalize this setting, following an idea presented in [5], we construct a metriplectic tensor that couples a Poisson structure with a pseudo-Riemannian structure. We introduce the generalized double bracket vector field and prove that in the particular case of a semi-simple Lie algebra it becomes the classical double bracket vector field.

In Section 3, we construct a pseudo-Riemannian metric on symplectic leaves, that we call double bracket metric. This generalizes the normal metric defined on an adjoint orbit of a compact semi-simple Lie algebra. Its construction is limited to good symplectic leaves, or more generally to green zones of symplectic leaves, notions that we define in the body of the paper. We then show that the restriction of the generalized double bracket vector field to a good symplectic leaf or a green zone in a symplectic leaf is the gradient of a smooth function with respect to this double bracket metric.

In Section 4, we provide a large class of Poisson structures on \mathbb{R}^3 and study their symplectic leaves. These include the Lie-Poisson manifold $\mathfrak{sl}(2, \mathbb{R})^*$ as well as a related

Poisson-Lie group. But they are much more general and, e.g., permit one to construct examples of symplectic leaves of arbitrary genus as explained in Section 5.

In Section 6, we introduce the pseudo-metric g which we put on the Poisson manifolds of the preceding section. This then permits us to discuss where problems with the non-degeneracy of g pulled back to symplectic leaves arise. We call the set R of such points the red zone, as it prohibits applying the constructions of Section 3.

In Section 7, the information about symplectic leaves gathered in Section 4 is combined with the one on the red zone. Intersecting a leaf S with R yields what we call red lines; the remainder of the leaf, $S \setminus (R \cap S)$, then provides the green zones. Leaves not having any such an intersection are simply good leaves. It is precisely the good leaves or, more generally, the green zones, where the Theorem 3.4 will be applicable. In the final Section 8 we compute the structures induced on the leaves for the class of our examples and illustrate Theorem 3.4 by means of them.

2. METRIPECTIC TENSOR. GENERALIZED DOUBLE BRACKET VECTOR FIELD

In this section we introduce the metriplectic tensor and the generalized double bracket vector field. These objects are constructed in a very general setting of a Poisson manifold (M, Π) endowed with a pseudo-Riemannian metric g , with no compatibility conditions required. We recover, as a particular case, the classical double bracket vector field.

We start by recalling the classical setting of the double bracket vector field. Let $(\mathfrak{g}, [\cdot, \cdot])$ be a semi-simple Lie algebra with $\kappa: \mathfrak{g} \times \mathfrak{g} \rightarrow \mathbb{R}$ the Killing form, hence a non-degenerate, symmetric, Ad-invariant bilinear form. The following vector field, called the double bracket vector field, has been introduced by Brockett [11], [12], see also [8], in the context of dynamical numerical algorithms and linear programming:

$$\dot{L} = [L, [L, N]], \quad (2.1)$$

where $L \in \mathfrak{g}$ and N is a fixed regular element in \mathfrak{g} . It turns out that the double bracket vector field is tangent to the adjoint orbits of the Lie algebra \mathfrak{g} , orbits that are the symplectic leaves for the linear Poisson bracket on \mathfrak{g} . More precisely, by identifying the Lie algebra \mathfrak{g} with its dual \mathfrak{g}^* using the Killing form, the Kirillov-Kostant-Souriau (KKS) Poisson bracket on \mathfrak{g}^* transforms into the linear Poisson bracket on \mathfrak{g} :

$$\{F, G\}_{\mathfrak{g}}(L) = \kappa(L, [\nabla F(L), \nabla G(L)]). \quad (2.2)$$

In the case of a compact semi-simple Lie algebra \mathfrak{g} , it has been proved that the double bracket vector field (2.1), when restricted to a regular adjoint orbit $S \subset \mathfrak{g}$, is a gradient vector field with respect to the normal metric. We recall briefly this construction, for details see [9], [10]. For every $L \in S$ consider the orthogonal decomposition with respect to the minus Killing form κ , that is $\mathfrak{g} = \mathfrak{g}_L \oplus \mathfrak{g}^L$, where $\mathfrak{g}_L = \text{Im}(\text{ad}_L)$ and $\mathfrak{g}^L = \text{Ker}(\text{ad}_L)$. The linear space \mathfrak{g}_L can be identified with the tangent space $T_L S$ and \mathfrak{g}^L with the normal space. One can endow the adjoint orbit S with the normal metric [4], also called standard metric [2],

$$\nu^S([L, X], [L, Y]) = -\kappa(X^L, Y^L), \quad (2.3)$$

where X^L, Y^L are the normal components according to the above orthogonal decomposition of X , respectively Y .

Theorem 2.1 ([9], [10]). *Let N be a fixed regular element in the compact semi-simple Lie algebra \mathfrak{g} . The gradient of the linear function $H: \mathfrak{g} \rightarrow \mathbb{R}$ defined by $H(L) = \kappa(L, N)$ restricted to a regular adjoint orbit S , taken with respect to the normal metric, is*

$$\nabla_{\nu^S}(H|_S)(L) = [L, [L, N]].$$

We move to a more general case: (M, Π, g) a Poisson manifold endowed with a pseudo-Riemannian metric.

Definition 2.1. *We call **metriplectic tensor** the following symmetric contravariant 2-tensor $\mathcal{M}: \Omega^1(M) \times \Omega^1(M) \rightarrow \mathcal{C}^\infty(M)$,*

$$\mathcal{M}(\alpha, \beta) := g(\sharp_{\Pi}\alpha, \sharp_{\Pi}\beta).$$

When $\alpha = dF$ and $\beta = dG$, where $F, G \in \mathcal{C}^\infty(M)$, we have

$$\mathcal{M}(dF, dG) = g(X_F, X_G).$$

Lemma 2.2. *The following identity $\sharp_{\mathcal{M}} = -\sharp_{\Pi} \circ \flat_g \circ \sharp_{\Pi}$ holds, where \flat_g is taken relative to the pseudo-Riemannian metric g on M .*

Proof. The proof is the following straightforward computation

$$\begin{aligned} (\sharp_{\mathcal{M}}\alpha)(\beta) &= \mathcal{M}(\alpha, \beta) = g(\sharp_{\Pi}\alpha, \sharp_{\Pi}\beta) = \sharp_{\Pi}\beta(\flat_g(\sharp_{\Pi}\alpha)) = \Pi(\beta, \flat_g \circ \sharp_{\Pi}(\alpha)) \\ &= -\Pi(\flat_g \circ \sharp_{\Pi}(\alpha), \beta) = -(\sharp_{\Pi} \circ \flat_g \circ \sharp_{\Pi})(\alpha)(\beta), \end{aligned}$$

for all $\alpha, \beta \in \Omega^1(M)$. □

In the finite dimensional case, the symmetric matrix associated to the contravariant tensor \mathcal{M} is given by

$$[\mathcal{M}] = [\Pi]^T[g][\Pi] = -[\Pi][g][\Pi]. \quad (2.4)$$

Metriplectic tensors similar with \mathcal{M} , that combine Poisson structures with Riemannian structures, have been previously introduced, for instance, in the works of J.P. Morrison [16, 17] and I. Vaisman [20].

We introduce the generalization of the double bracket vector field on a nonlinear Poisson manifolds.

Definition 2.2. Let (M, g, Π) be a pseudo-Riemannian manifold equipped with a Poisson structure. For a smooth function G on M , we call the vector field

$$\partial_{\mathcal{M}}G := -i_{dG}\mathcal{M}, \quad (2.5)$$

the **generalized double bracket vector field**.

Remark 2.1. By Lemma 2.2, one sees that the generalized double bracket vector field $\partial_{\mathcal{M}}G$ is closely related to the Hamiltonian vector field X_G . For $G \in \mathcal{C}^\infty(M)$, we have

$$\partial_{\mathcal{M}}G = (\sharp_{\Pi} \circ \flat_g)(X_G) = i_{\flat_g(X_G)}\Pi, \quad (2.6)$$

hence $\partial_{\mathcal{M}}G$ is tangent to all the symplectic leaves of Π . Note also that $\partial_{\mathcal{M}}G = -\sharp_{\mathcal{M}}(dG)$ by (2.5).

The vector field $\partial_{\mathcal{M}}G$ is a natural generalization of the double bracket vector field defined on a semi-simple Lie algebra \mathfrak{g} . The Killing form provides an isomorphism $b_{\kappa}: \mathfrak{g} \rightarrow \mathfrak{g}^*$ which transports the Poisson structure from \mathfrak{g}^* to the linear Poisson structure on \mathfrak{g} in (2.2).

Lemma 2.3. *On the semi-simple Lie algebra \mathfrak{g} , with the linear Poisson structure (2.2), the Hamiltonian vector field with Hamiltonian function $G \in C^{\infty}(\mathfrak{g})$ is*

$$X_G(L) = [L, \nabla G(L)], \text{ for all } L \in \mathfrak{g}, \quad (2.7)$$

where the gradient is taken with respect to the Killing metric κ on \mathfrak{g} .

Proof. The Hamiltonian vector fields with Hamiltonian functions G and $\bar{G} = G \circ \sharp_{\kappa}$ on \mathfrak{g}^* are κ -related, hence it is enough to show that the Hamiltonian vector field $X_{\bar{G}}$ is

$$X_{\bar{G}}(\xi) = \kappa([L, \nabla G(L)]), \text{ for all } \xi = b_{\kappa}(L) \in \mathfrak{g}^*.$$

By the definition of the Lie-Poisson bracket on \mathfrak{g}^* :

$$\Pi_{\xi}(L, L') = (\xi, [L, L'])$$

for all $L, L' \in \mathfrak{g} \cong \mathfrak{g}^{**}$. Thus, for $\xi = b_{\kappa}(L)$,

$$\Pi_{\xi}(\nabla G(L), L') = (\xi, [\nabla G(L), L']) = \kappa(L, [\nabla G(L), L']) = \kappa([L, \nabla G(L)], L'). \quad (2.8)$$

On the other hand, the Hamiltonian vector field with Hamiltonian function \bar{G} satisfies

$$\Pi_{\xi}(d\bar{G}(\xi), L') = (X_{\bar{G}}(\xi), L'). \quad (2.9)$$

Since $\nabla G(L) = d\bar{G}(\xi)$, where $d\bar{G}(\xi) \in \mathfrak{g}^{**} = \mathfrak{g}$, the identity (2.7) follows from (2.8) and (2.9). \square

Theorem 2.4. *Let $(\mathfrak{g}, [\cdot, \cdot])$ be a semi-simple Lie algebra endowed with the Poisson bracket defined by (2.2). Then the nonlinear double bracket vector field coincides with the classical double bracket vector field:*

$$\partial_{\mathcal{M}}G(L) = [L, [L, \nabla G(L)]].$$

Proof. As before, we work on \mathfrak{g}^* , so let $\xi = b_{\kappa}(L)$. The formula (2.6) implies

$$\begin{aligned} (\partial_{\mathcal{M}}\bar{G}(\xi), L') &= \Pi_{\xi}(b_{\kappa}(X_{\bar{G}})(\xi), L') = \Pi_{\xi}(X_G(L), L') = (\xi, [X_G(L), L']) \\ &= \kappa(L, [X_G(L), L']) = \kappa([L, X_G(L)], L'), \end{aligned}$$

hence $\partial_{\mathcal{M}}\bar{G}(b_{\kappa}(L)) = \kappa([L, X_G(L)])$. By using the fact that the nonlinear double bracket vector fields on \mathfrak{g} and \mathfrak{g}^* are κ -related, we get $\partial_{\mathcal{M}}G(L) = [L, X_G(L)]$. Now the Lemma 2.3 yields the conclusion. \square

3. GRADIENT NATURE OF THE GENERALIZED DOUBLE BRACKET VECTOR FIELD

In this section, we prove that the generalized double bracket vector field defined in Definition 2.2, when restricted to a leaf, is a gradient vector field with respect to a metric, that we call double bracket metric. This metric generalizes the normal metric defined on the regular adjoint orbits of a semi-simple compact Lie algebra. In the case when the ambient metric is of indefinite signature, one has to be careful when dealing

with submanifolds as they might not be pseudo-Riemannian with respect to the induced metric [19].

As a consequence of Lemma 2.2, we have the inclusion $\text{Im } \sharp_{\mathcal{M}} \subseteq \text{Im } \sharp_{\Pi}$. Points where the two images do not coincide merit special attention:

Definition 3.1. A point $m \in M$ is called \mathcal{M} -**regular** if $\text{Im } \sharp_{\Pi}|_m = \text{Im } \sharp_{\mathcal{M}}|_m$ and m is called \mathcal{M} -**singular** otherwise.

Proposition 3.1. *Let S denote a symplectic leaf of (M, g, Π) and $\iota: S \hookrightarrow M$. Then the two-tensor $g_{\text{ind}}^S := \iota^*g$ induced by g on S is degenerate at $s \in S$ if and only if s is \mathcal{M} -singular.*

Proof. Since $\sharp_{\Pi}: T^*M \rightarrow TS$ is surjective, g_{ind}^S is non-degenerate iff $g_{\text{ind}}^S(\sharp_{\Pi}\alpha, \sharp_{\Pi}\beta) = 0$ for all $\beta \in T^*M$ implies $\alpha \in \ker \sharp_{\Pi}$. The induced metric g_{ind}^S coincides with g upon evaluation on vectors tangent to S . By Definition 2.1, one has

$$g_{\text{ind}}^S(\sharp_{\Pi}\alpha, \sharp_{\Pi}\beta) = \beta(\sharp_{\mathcal{M}}\alpha),$$

for all $\alpha, \beta \in T^*M$. The right-hand-side vanishes for all $\beta \in T^*M$ iff $\alpha \in \ker \sharp_{\mathcal{M}}$. Consequently, g_{ind}^S is degenerate iff $\text{Ker } \sharp_{\Pi} \subsetneq \text{Ker } \sharp_{\mathcal{M}}$. This is equivalent with the strict inclusion $\text{Im } \sharp_{\mathcal{M}} \subsetneq \text{Im } \sharp_{\Pi}$, hence the conclusion. \square

Remark 3.1. For a Riemannian metric g , all points in M are \mathcal{M} -regular. In particular, the \mathcal{M} -distribution $\text{Im } \sharp_{\mathcal{M}}$ coincides with the characteristic distribution of the Poisson manifold, hence it is integrable. On the other hand, in the case of a pseudo-Riemannian metric g with signature, the integrability of this \mathcal{M} -distribution is not guaranteed.

Definition 3.2. We call a symplectic leaf $S \subset M$ a **good symplectic leaf** if the induced metric g_{ind}^S is non-degenerate. Equivalently, S is a good symplectic leaf if all its points are \mathcal{M} -regular.

Example 3.1. Consider $M = \mathbb{R}^4 \ni (w, x, y, z)$ equipped with the pseudo-Riemannian metric¹ $g = 2dw dx + 2dy dz$ and the Poisson bivector field $\Pi := \partial_x \wedge \partial_y$. Every symplectic leaf S is a plane characterized by $w = w_0, z = z_0$ for some $(w_0, z_0) \in \mathbb{R}^2$. Here, on every S , the induced metric vanishes identically,

$$g_{\text{ind}}^S = 0,$$

since $dw|_S = 0$ and $dz|_S = 0$. Correspondingly, as a direct matrix calculation shows easily, see (2.4), the metriplectic tensor vanishes identically as well, $\mathcal{M} = 0$, so that $\text{Im } \sharp_{\mathcal{M}} = \{0\} \neq \text{Vect}(\partial_x, \partial_y) = \text{Im } \sharp_{\Pi}$. Every point $m \in \mathbb{R}^4$ is \mathcal{M} -singular. All leaves are bad in this example.

In what follows we will define the double bracket metric on a good symplectic leaf and we will prove that this metric generalizes the normal/standard metric on adjoint orbits of a semi-simple compact Lie algebra. However, all the statements below will be applicable also to \mathcal{M} -regular regions of a symplectic leaf S , called **green zones** in Section 6 below.

¹We omit writing the symmetrized tensor product, so, e.g., $2dw dx$ stands for $dw \otimes dx + dx \otimes dw$.

In analogy with the compact semi-simple Lie algebra case, we have the following result.

Theorem 3.4. *Let M be a smooth manifold equipped with a pseudo-Riemannian structure and with a Poisson structure. On a good symplectic leaf S , the generalized double bracket vector field $\partial_M G$, for $G \in C^\infty(M)$, is minus the gradient vector field of $G|_S$ with respect to the double bracket metric:*

$$(\partial_M G)(x) = -\nabla_{\tau_{\text{DB}}^S} (G|_S)(x), \quad x \in S. \quad (3.2)$$

Proof. Using the Lemma 3.3, we have,

$$\begin{aligned} (\partial_M G)|_S &= (\sharp_M(dG))|_S = \iota_* \sharp_{\tau_{\text{DB}}^S} (\iota^*(dG)|_S) \\ &= \iota_* \sharp_{\tau_{\text{DB}}^S} (d(G|_S)) = -\iota_* \nabla_{\tau_{\text{DB}}^S} (G|_S), \end{aligned}$$

hence the equality in (3.2). \square

Next, we will show that for the case of a compact semi-simple Lie algebra the double bracket metric introduced above and the normal metric (2.3) coincide up to a sign.

Theorem 3.5. *Let \mathfrak{g} be a semi-simple compact Lie algebra and let S be a regular adjoint orbit in \mathfrak{g} . Then*

$$\tau_{\text{DB}}^S = -\nu^S.$$

Proof. Compactness implies that the Killing form has index zero, thus every symplectic leaf S of \mathfrak{g} is a good symplectic leaf.

It is enough to show that for all the functions on $S \subset \mathfrak{g}$ of the form $H(L) = \kappa(L, N)$, with N regular element in S , the gradient taken with respect to the normal metric ν^S is the opposite of the gradient taken with respect to the double bracket metric τ_{DB}^S . By Theorem 2.1 we have $\nabla_{\nu^S} H(L) = [L, [L, N]]$ for all $L \in S$. On the other hand, by Theorem 2.4, we also have $\partial_M H(L) = [L, [L, \nabla H(L)]] = [L, [L, N]]$. Combined with Theorem 3.4, it yields that $\nabla_{\nu^S} H(L) = -\nabla_{\tau_{\text{DB}}^S} H(L)$, thus $\nu^S = -\tau_{\text{DB}}^S$. \square

4. A CLASS OF POISSON STRUCTURES ON \mathbb{R}^3 AND THEIR SYMPLECTIC LEAVES

In this section we work with a large class of Poisson structures on \mathbb{R}^3 that illustrate all the new notions introduced in the previous sections. Among them, we specify three examples of a linear Poisson structure, a quadratic Poisson structure and a Poisson Lie group. Symplectic leaves and green zones of each case, where our main theorem is applicable, are carefully studied in the next sections.

The canonical basis of the Lie algebra $\mathfrak{sl}(2, \mathbb{R})$,

$$\mathbf{e}_1 = \begin{pmatrix} 0 & 1 \\ 0 & 0 \end{pmatrix}, \quad \mathbf{e}_2 = \begin{pmatrix} 0 & 0 \\ 1 & 0 \end{pmatrix}, \quad \mathbf{e}_3 = \begin{pmatrix} 1 & 0 \\ 0 & -1 \end{pmatrix},$$

gives rise to the standard form of its Lie brackets:

$$[\mathbf{e}_1, \mathbf{e}_2] = \mathbf{e}_3; \quad [\mathbf{e}_1, \mathbf{e}_3] = -2\mathbf{e}_1; \quad [\mathbf{e}_2, \mathbf{e}_3] = 2\mathbf{e}_2. \quad (4.1)$$

They induce a linear Poisson structure on the dual. More precisely, rescaling the basis elements, $x := \mathbf{e}_1/\sqrt{2}$, $y := \mathbf{e}_2/\sqrt{2}$, and $z := \mathbf{e}_3/2$, and considering them as coordinates on the dual $\mathfrak{sl}(2, \mathbb{R})^* \cong \mathbb{R}^3$, we get

$$\{x, y\}_{\text{lin}} = z, \quad \{z, x\}_{\text{lin}} = x, \quad \{z, y\}_{\text{lin}} = -y. \quad (4.2)$$

These can be considered as the fundamental Poisson brackets on \mathbb{R}^3 , extended to all smooth functions by means of the Leibniz rule.

We now consider the following non-linear generalization of these brackets:

$$\{x, y\} = U(z) + V(z)xy, \quad \{z, x\} = x, \quad \{z, y\} = -y, \quad (4.3)$$

where U and V are arbitrarily chosen smooth functions. For the choice $U = \text{id}$ and $V = 0$ we regain the formulas (4.2). It is easy to verify that (4.3) satisfies the Jacobi identity and thus defines a Poisson structure. Such Poisson structures appeared in the study of two-dimensional gravity models [15].

A nice feature of these brackets is that a Casimir function, a non-constant function in the center of the Poisson bracket, can be found explicitly:

Lemma 4.1 ([15]). *Let P be a primitive of the function V , $P'(z) = V(z)$, and Q such that $Q'(z) = U(z) \exp(P(z))$. Then the function $C \in C^\infty(\mathbb{R}^3)$ defined by*

$$C(x, y, z) := xy \exp(P(z)) + Q(z) \quad (4.4)$$

is a Casimir function of the brackets (4.3).

The generic symplectic leaves are obtained simply from putting C equal to some constant $c \in \mathbb{R}$, $C(x, y, z) := c$. This will permit us to visualize the leaves in different cases.

While the generic leaves are two-dimensional, there are also point-like singular leaves. They occur when the right-hand side of (4.3) vanishes, i.e. when $(x, y) = (0, 0)$ and z is a zero of the function U . The singular symplectic leaves are thus restricted to the z -axis and lie at such values of z . Let us denote the union of all singular symplectic leaves of (M, Π) by

$$\mathcal{L}_{\text{sing}} := \{(0, 0, z) \in \mathbb{R}^3 \mid U(z) = 0\}. \quad (4.5)$$

All other leaves are regular.

Let us now depict some of the symplectic leaves in particular cases:

Example 4.1 (Linear brackets). For the brackets (4.2), the Casimir function (4.4) becomes

$$C_{\text{lin}}(x, y, z) = xy + \frac{1}{2}z^2. \quad (4.6)$$

To plot some of its well-known level surfaces, it is convenient to use the coordinates

$$X := z, \quad Y := \frac{x+y}{\sqrt{2}}, \quad T := \frac{x-y}{\sqrt{2}} \quad (4.7)$$

which gives

$$2C_{\text{lin}} = X^2 + Y^2 - T^2. \quad (4.8)$$

In this example, there is precisely one singular symplectic leaf, which lies at the origin. The level surface $C_{\text{lin}} = c$ for $c = 0$ splits into three leaves, the singular leaf at the origin and the two cones² with $T > 0$ and $T < 0$, which are regular leaves. Choosing $c > 0$, we obtain a one-sheeted hyperboloid, which topologically is a cylinder while for $c < 0$ we obtain the two-sheeted hyperboloids, two regular leaves of trivial topology each. See Fig. 1 for an illustration.

²We still call them ‘‘cones’’ despite of that the tips are not included.

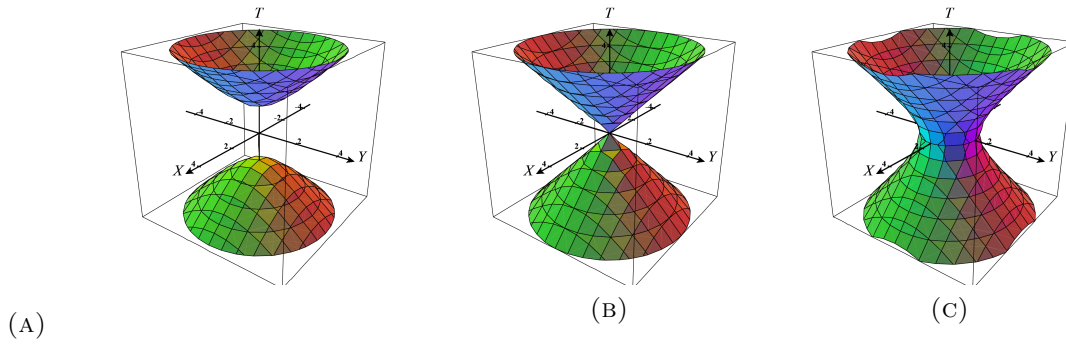


FIGURE 1. Symplectic leaves on $\mathfrak{sl}(2, \mathbb{R})^*$: (A) for $c = -1$, (B) for $c = 0$, and (C) for $c = 1$

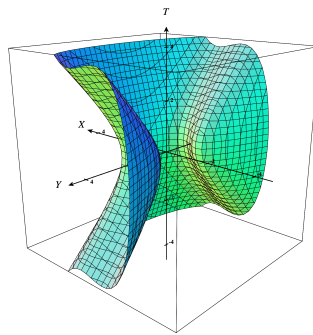


FIGURE 2. Quadratic bracket: symplectic leaf for $c = 1$

As special non-linear cases of (4.3), we first consider the following one:

Example 4.2 (Quadratic brackets). With the choice

$$U_{\text{qua}}(z) := 3z^2 - 1 \quad , \quad V_{\text{qua}}(z) := 0 \quad , \quad (4.9)$$

one obtains quadratic brackets from (4.3). The Casimir (4.4) takes the form

$$C_{\text{qua}} = xy + z^3 - z \quad , \quad (4.10)$$

when choosing $P = 0$ and $Q = z^3 - z$. (Changing the integration constants for P and Q , leads to the (irrelevant) redefinition $C_{\text{qua}} \mapsto e^a C_{\text{qua}} + b$ for some $a, b \in \mathbb{R}$).

There are now precisely two singular leaves, at $(0, 0, \frac{1}{\sqrt{3}})$ and $(0, 0, -\frac{1}{\sqrt{3}})$, as $\pm \frac{1}{\sqrt{3}}$ are the two zeros of the function U , cf. (4.9). These happen for the critical values $c = \pm 2\sqrt{3}$ of the Casimir function, which implies that the level set splits into regular and singular leaves for those values. For all other values we have two-dimensional and thus regular symplectic leaves. If we choose $c = 1$, for example, we obtain a topologically trivial symplectic leaf, depicted in Fig. 2. On the other hand, for $c = 0$, we find a symplectic leaf with two holes, i.e. essentially two cylinders orthogonal to one another glued together to form a single leaf—see Fig. 3. Now, topologically, S is a genus one surface with one puncture.

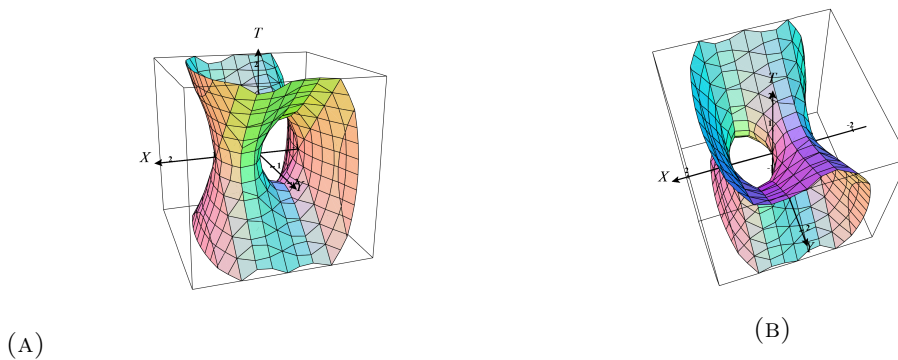


FIGURE 3. Quadratic bracket: symplectic leaf S for $c = 0$: (A) seen from the side (B) seen from above. Topologically S is a punctured torus.

We finally also provide an example where the function V is non-zero:

Example 4.3 (Poisson-Lie group [3]³). Consider the three-dimensional *book Lie algebra* $\tilde{\mathfrak{g}}$, described by the Lie brackets $[\tilde{z}, \tilde{x}] = -\eta\tilde{x}$, $[\tilde{z}, \tilde{y}] = -\eta\tilde{y}$, and $[\tilde{x}, \tilde{y}] = 0$ for some appropriate choice of generators \tilde{x} , \tilde{y} , and \tilde{z} and a non-vanishing real parameter η , whose significance will become visible shortly. The couple $(\tilde{\mathfrak{g}}, \mathfrak{sl}(2, \mathbb{R}))$ forms a well-known Lie bialgebra. Integrating $\tilde{\mathfrak{g}}$ to its unique connected and simply connected Lie group \mathcal{G} thus leads to a Poisson-Lie group. It turns out that, as a manifold, $\mathcal{G} \cong \mathbb{R}^3$, and its Poisson structure is given by (4.3) for the choice

$$U_{\text{grp}}(z) := \frac{1 - e^{-2\eta z}}{2\eta} \quad , \quad V_{\text{grp}}(z) := \eta. \quad (4.11)$$

We now see that η can be considered as a deformation parameter here: in the limit of sending η to zero, we get back the linear brackets (4.2). For an appropriate choice of integration constants, (4.4) yields

$$C_{\text{grp}} = xye^{\eta z} + \frac{\cosh(\eta z) - 1}{\eta^2} \quad (4.12)$$

which also reduces to the $\mathfrak{sl}(2, \mathbb{R})$ -Casimir (4.6) in the limit. This example provides a particularly interesting 1-parameter family of deformations of the linear Poisson structure on $\mathfrak{sl}(2, \mathbb{R})^*$ within the infinite-dimensional deformation space governed by the two functions U and V as it corresponds to a Poisson-Lie group.

5. TOPOLOGICAL NATURE OF CERTAIN SYMPLECTIC LEAVES

To better understand the topological nature of the symplectic leaves for different choices of U and c , still keeping V zero for simplicity, it is convenient to consider the following function:

$$h_c(z) := Q(z) - c. \quad (5.1)$$

The number and kind of zeros of this function determines the topology.

³For an easier comparison with [3], use the coordinates $x_1 := z$, $x_2 := \sqrt{2}y$, and $x_3 := \sqrt{2}x$ in the formulas below and rescale C_{grp} by a factor of $\frac{1}{2}$.

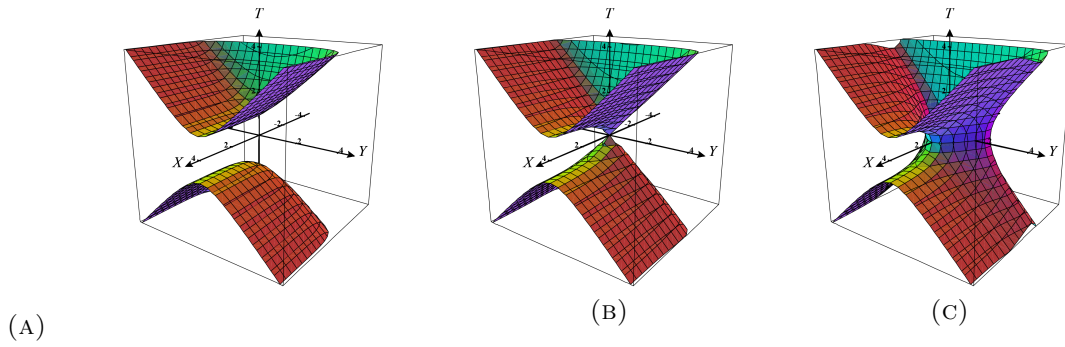


FIGURE 4. Symplectic leaves on Poisson-Lie group for the deformation parameter $\eta = 1$: (A) for $c = -1$, (B) for $c = 0$, and (C) for $c = 1$. For $\eta \rightarrow 0$, they more and more approach the leaves shown in Fig. 1.

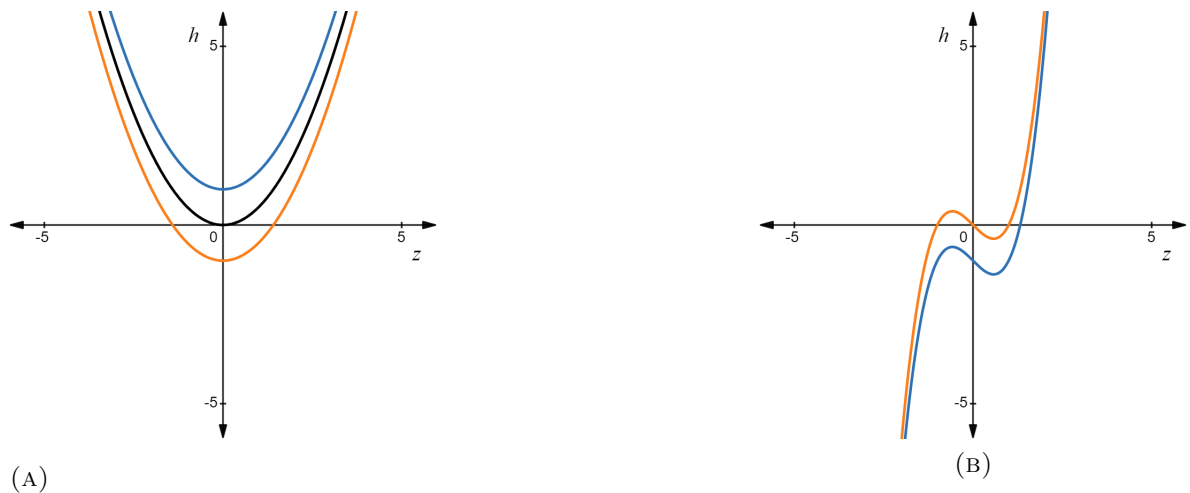


FIGURE 5. (A) Function h_c for the linear Poisson structure on $\mathfrak{sl}(2, \mathbb{R})^*$, orange color for h_{-1} , black color for h_0 and blue color for h_1 . (B) Function h_c for the quadratic Poisson structure, orange color for h_0 and blue color for h_1 .

Let us first consider Example 4.1, where we depict this function for the three values $c = -1$, $c = 0$, and $c = +1$ in Fig. 5A. We see that h_{-1} has no zeros and that the corresponding leaf is topologically trivial, cf. Fig. 1A, while h_1 has two simple roots and the leaf S for $c = 1$ is a cylinder topologically. This qualitative behaviour of h_c and the corresponding leaves remains if one does not change the sign of c . For the special value $c = 0$, on the other hand, we have one multiple root of this function and precisely there we find a singular leaf together with two regular ones.

In fact, the latter observation is not a coincidence: Recall that all singular leaves lie on the z - or X -axis for values where the function U vanishes, see (4.5). By the definition (5.1), we see that for every value of z where U vanishes also h'_c vanishes. So singular leaves appear for values of c where h_c has a multiple zero.

Let us now look at the second example, Example 4.2, and depict the graph of h_1 and h_0 —see Fig. 5B. For $c = 1$ the function has one simple zero and the leaf is a plane topologically. For $c = 0$, the function has three simple zeros and the corresponding leaf S the fundamental group $\pi_1(S) = \mathbb{F}_2$, the free group with two generators.

More generally, the situation is as follows. If the function h_c has $n \geq 1$ simple zeros, then S is a Riemann surface of genus $\lfloor \frac{n+1}{2} \rfloor - 1$, where the square brackets denote the integer part of the enclosed number, with one puncture if n is odd and two punctures if n is even. So, for $n = 3$ we obtain a punctured torus, in agreement with what we had found above for its fundamental group. For $n = 4$ we get a torus with two punctures (boundary components)—see Fig. 6, while for $n = 5$ already a genus two surface with one puncture—see Fig. 7. Such leaves arise, for example, if we take $Q(z) = 2(z-2)(z-1)(z+1)(z+2)$ and $Q(z) = 2(z-2)(z-1)z(z+1)(z+2)$, respectively, and choose $c = 0$ (so that $h_0 = Q$). By reverse engineering, the Poisson brackets yielding such leaves can be obtained from the brackets (4.3) when choosing $U = Q'$ and $V = 0$. For completeness, we mention that if h_c has no zeros, one obtains two planar symplectic leaves, and if it has zeros of some multiplicity, the leaf contains singular ones.

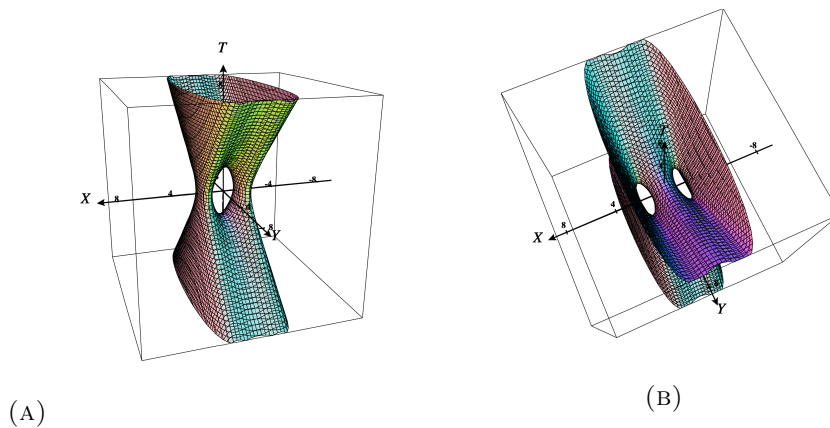


FIGURE 6. The symplectic leaf when $h(z) = 2(z-2)(z-1)(z+1)(z+2)$, in (A) from the side and in (B) from above. Topologically it is a genus one surface with two punctures or boundary components.

Evidently, the freedom in choosing the function U in the brackets (4.3) permits one to obtain much more intricate symplectic leaves than in the linear case shown in Figure 1. Fixing any integer $k \in \mathbb{N}$, by an appropriate choice U , we can create a sample of symplectic leaves which topologically are Riemann surfaces of genus k —with optionally one or two boundary components.

6. DEGENERACY STRUCTURE OF THE METRIPECTIC TENSOR: RED ZONES

The second main ingredient is the choice of a metric on the space where the leaves are embedded in, i.e. here on the Poisson manifold \mathbb{R}^3 . In the case of the linear $\mathfrak{sl}(2, \mathbb{R})^*$ brackets, there is a natural candidate for such a metric, the Killing metric κ of the Lie

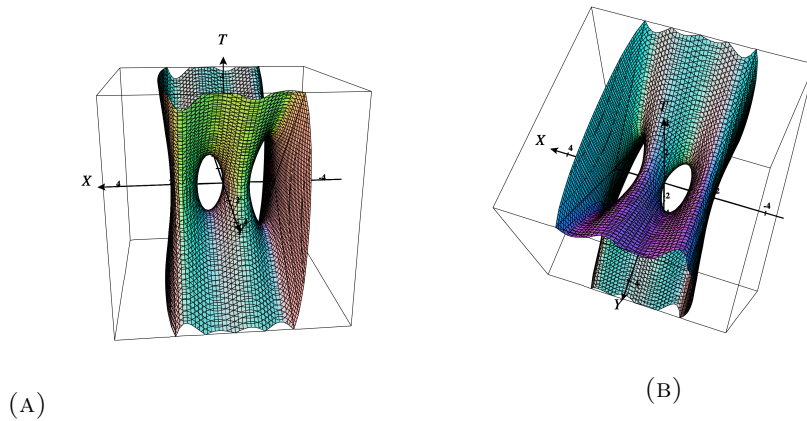


FIGURE 7. The symplectic leaf when $h(z) = 2(z-2)(z-1)z(z+1)(z+2)$, in (A) from the side and in (B) from above. Topologically it is a punctured genus two surface.

algebra $\mathfrak{sl}(2, \mathbb{R})$. It is of indefinite signature, corresponding to the fact that $SL(2, \mathbb{R})$ is a non-compact Lie group. After a trivial rescaling, $g := \frac{1}{2}\kappa$, this metric takes the form

$$g = 2 dx dy + dz^2 = -dT^2 + dX^2 + dY^2, \quad (6.1)$$

written in both of the coordinate systems used before. Recall that we omit writing the symmetrized tensor product; correspondingly, dz^2 stands for $dz \otimes dz$.

As mentioned in the introduction, we do not want to make a sophisticated choice for the metric on the given Poisson manifold, potentially one that would adapt to the symplectic leaves of the given Poisson structure, for example. The metric should be simple and thus we do not also deform (6.1) along with the brackets.

The metric (6.1) allows us to identify the given \mathbb{R}^3 with a 2+1 dimensional Minkowski space, T being a time coordinate and X and Y spatial coordinates. To decide in a case by case study where the potential metric g^S induced by g on a given symplectic leaf becomes degenerate, may be cumbersome. In general, one needs an atlas to cover such a leaf—even in the case of the two-dimensional leaves under consideration here. Therefore, one needs to see if a degeneracy of g^S in some coordinate system on the leaf is due to an intrinsic degeneracy or happens because of a bad choice of coordinates (like when writing the standard metric on \mathbb{R}^2 in polar coordinates). Fortunately, this is not necessary.

Using the Definition 2.1 or, equivalently, Equation (2.4), the matrix corresponding to the metriplectic tensor \mathcal{M} in the basis $\partial_x \otimes \partial_x, \partial_x \otimes \partial_y, \dots, \partial_z \otimes \partial_z$ takes the form

$$[\mathcal{M}] = \begin{pmatrix} x^2 & -xy - W^2 & xW \\ -xy - W^2 & y^2 & yW \\ xW & yW & -2xy \end{pmatrix} \quad (6.2)$$

where we introduced the abbreviation

$$W = U(z) + xy V(z). \quad (6.3)$$

Proposition 6.1. *Let (\mathbb{R}^3, g, Π) be one of the pseudo-Riemannian Poisson manifolds considered in this section. The points $m = (x, y, z) \in \mathbb{R}^3$ for which the function*

$$f(x, y, z) := 2xy + W^2(x, y, z) \tag{6.4}$$

vanishes are precisely the points of one of the two classes below:

- m is an \mathcal{M} -singular point
- $\{m\}$ is a singular symplectic leaf.

Proof. We always have $\text{Im } \sharp_{\mathcal{M}} \subseteq \text{Im } \sharp_{\Pi}$. Thus whenever Π_m vanishes—i.e. at the points $m \in \mathcal{L}_{\text{sing}}$ —also \mathcal{M}_m does. But there are no further points where \mathcal{M} vanishes, as inspection of (6.2) shows. Since (6.4) vanishes at these points, too, we proved the second item in the proposition.

It remains to show that all the remaining points $m \in \mathbb{R}^3$ for which f vanishes are those where $\text{rk } \mathcal{M}_m = 1$. First let us show that the condition is sufficient: Replacing $-(xy+W^2)$ by xy in the first two lines and $-2xy$ by W^2 in the third line, we see that each of the three lines is proportional to $(x \ y \ W)$. So, at points where (6.4) vanishes, the rank of \mathcal{M} is one.

To see that $f = 0$ is also necessary for $\text{rk } \mathcal{M}_m = 1$, note first that if both x and y vanish, then the rank of \mathcal{M} cannot be odd. Suppose first then that $x \neq 0$: Subtract the first line multiplied by $\frac{1}{x}W$ from the third. Then the new third line becomes $(0 \ * \ f)$. So, $f = 0$ is necessary for rank one of \mathcal{M} in this case. A similar argument for $y \neq 0$ —or noting that \mathcal{M} remains unchanged under the diffeomorphism $(x, y, z) \mapsto (y, x, z)$ —provides the same result. \square

The pseudo-Riemannian Poisson manifolds (M, g, Π) considered in this section are defined by $M = \mathbb{R}^3$, the pseudo-Riemannian metric (6.1), and the bivector (cf. (4.3))

$$\Pi = W(x, y, z) \partial_x \wedge \partial_y - x \partial_x \wedge \partial_z + y \partial_y \wedge \partial_z, \tag{6.5}$$

where the function W is given in (6.3) and U and V can be chosen arbitrarily. Our main theorem, Theorem 3.4, is applicable whenever we exclude \mathcal{M} -singular points, while singular symplectic leaves—all pointlike in our case, see (4.5)—are admissible. Thus, in view of Prop. 6.1, let us define the set

$$R := \{(x, y, z) \in \mathbb{R}^3 \mid f(x, y, z) = 0\} \setminus \mathcal{L}_{\text{sing}}, \tag{6.6}$$

with $\mathcal{L}_{\text{sing}}$ defined in (4.5). More explicitly, the function f is given by

$$f(x, y, z) = U^2 + 2(1 + UV)xy + V^2(xy)^2, \tag{6.7}$$

where U and V depend on z only. R is a smooth manifold. We will henceforth call R the *red zone* of the given triple (M, g, Π) .

Let us illustrate this for the three examples highlighted in Section ??:

Example 6.1. For the case $(\mathfrak{sl}(2, \mathbb{R})^*, \kappa, \Pi_{\mathfrak{sl}(2, \mathbb{R})^*})$ of Example 4.1, resulting from $U(z) = z$ and $V = 0$ in (6.5), we see that $f(x, y, z) = 2C(x, y, z)$, cf. (4.6). Thus, the red zone R , depicted in Fig. 8A, agrees precisely with the two regular symplectic leaves obtained from $C_{\text{lin}} = 0$ when the origin is excluded, see Fig. 1B. Both these leaves are thus “bad” symplectic leaves.

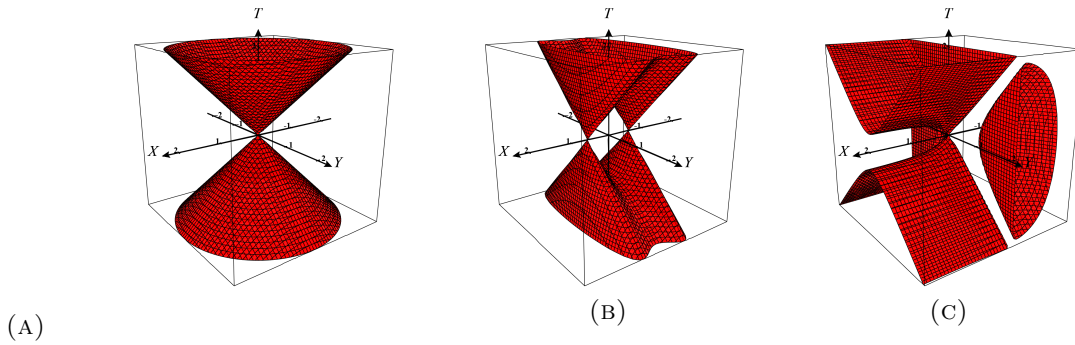


FIGURE 8. The red zones R for the three main examples, all with respect to the metric g in (6.1):

(A) The Lie Poisson manifold $\mathfrak{sl}(2, \mathbb{R})^*$, Example 4.1,

(B) Example 4.2 with the bivector Π_{qua} , cf. (6.8), and

(C) the Poisson-Lie group of Example 4.3 for the choice $\eta := 1$.

In all three cases, R is invariant under $Y \rightarrow -Y$ as well as, separately, under $T \rightarrow -T$. In (A) and (B), R has two connected components—recall the the singular leaves, all at the conic tips of the red surfaces, do not belong to R . In (C), R has four connected components

That, for a generic choice of U and V , symplectic leaves are not entirely included in the forbidden red zones becomes well obvious already when looking at the function f for Example 4.2. The corresponding surface R is drawn in Fig. 8B and has more or less nothing to do with symplectic leaves of the Poisson bivector

$$\Pi_{qua} = (3z^2 - 1) \partial_x \wedge \partial_y - x \partial_x \wedge \partial_z + y \partial_y \wedge \partial_z, \quad (6.8)$$

depicted in Figs. 2 and 3 for two values of the Casimir function. As mentioned in the general discussion above, R does not contain the singular leaves. For the bivector (6.8), these lie at $(x, y, z) = (0, 0, \pm \frac{1}{\sqrt{3}})$, corresponding to $X = \pm \frac{1}{\sqrt{3}}$, $Y = 0$ and $T = 0$. These two points are well visible in Fig. 8B; they coincide with the conic tips of the red surface, to which they do not belong.

The red zones for Example 4.3, the Poisson-Lie group, are drawn in Fig. 8C. They are already quite intricate to imagine graphically and it is not obvious at first sight, if not some of the symplectic leaves, such as those depicted in Fig. 4, would lie inside the four connected components of R . That this is not the case becomes evident when looking at the intersection with the symplectic leaves of (M, Π_{grp}) : The intersection of the three leaves of Fig. 4 with R is depicted in Fig. 9.

7. GEOMETRIC INTERPRETATION, GREEN ZONES AND RED LINES

There is a geometrical way of seeing from the pictures if a leaf S or a region inside S carries a non-degenerate induced metric. And this is the main reason, why we used the coordinates X , Y , and T for the pictures in this section—still keeping x , y , and z for the calculations, as they are somewhat more convenient there. With the “causal coordinates” (X, Y, T) , we identify M with the 2+1-dimensional “Minkowski space” $\mathbb{R}^3 = \{(X, Y, T)\}$.

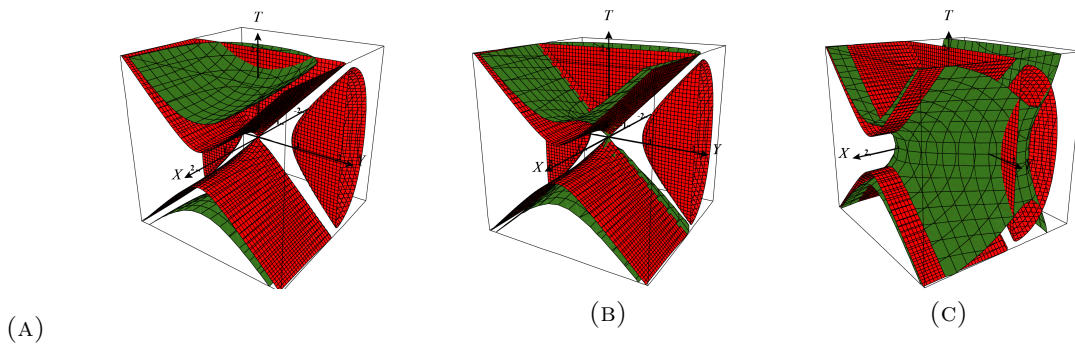


FIGURE 9. Intersecting the red zone R of the Poisson Lie group, drawn in red for $\eta = 1$, with the three symplectic leaves obtained for (A) $c = -1$, (B) $c = 0$, and (C) $c = 1$, all drawn in green.

Then the three symplectic leaves in Fig. 1 receive the following reinterpretation. The one with $T > 0$ is the “future light cone”, the one with $T < 0$ the “past light cone”. They are separated by “present time”, the pointlike symplectic leaf at $(0, 0, 0)$.

Let us now recall some basic facts and terminology from Minkowski space M : A vector $v \in TM$ is called *time-like* if its “length” (squared) is negative, $g(v, v) < 0$, *space-like* if $g(v, v) > 0$, and *null*, if $g(v, v) = 0$. Vectors are time-like if they “essentially vertical” in our drawings, i.e. if they have an angle less than 45 degrees with respect to the the T -axis, they are null, if this angle is precisely 45 degrees, and space-like if they are “essentially horizontal” (angle bigger than 45 degrees). A curve is called time-like, space-like or null, if all its tangent vectors are of the corresponding nature.

A submanifold or part of a submanifold S is of Riemannian or Euclidean nature—the induced metric g_{ind}^S is positive definite—if all curves lying inside S are space-like. This is, for example, evidently the case for Fig. 1A, but also applies to all the yellow parts in the leaves of Fig. 4. Now, a submanifold S , or a part of it, is pseudo-Riemannian or Lorentzian, if, at every of its points s , it contains curves passing through s that are spacelike and (other) such curves that are timelike. This applies, e.g., to the symplectic leaf depicted in Fig. 2, but also to at least part of the light green regions in the leaves of Fig. 4. Thus, for example, the leaf S depicted in Fig. 3 contains Euclidean regions—at least at the bottom and top of the hole visible in Fig. 3A—as well as Lorentzian regions—like the left side of Fig. 3A. Due to the signature change needed for this to happen, there must be lines, which we will call *red lines*, where the signature change happens and where thus necessarily the induced bilinear form g_{ind}^S must be degenerate.

For completeness we return also to the future and past light cones, see Fig. 1B and Fig. 8A: Through every point m on them, there is a null-curve (consider the straight line connecting the origin with m), there are also plenty of space-like curves. However, there is no time-like curve passing through m . So the zero length of the null tangent vector can be explained there only by the fact that such a vector becomes an eigenvector with eigenvalue zero of the induced bilinear form g_{ind}^S at m . We deal with entirely bad leaves in this case.

It is obvious from the above qualitative discussion, however, that leaves which are \mathcal{M} -singular *everywhere* (“bad leaves”) are very exceptional. More often they will be either good leaves—leaves which do not have an intersection with the red zone R —or leaves of mixed nature, where Lorentzian and Euclidean regions are separated by red lines of \mathcal{M} -degenerate points.⁴

Let us illustrate this by means of Example 4.2: Fig. 2 shows a leaf S that is endowed with a Lorentzian metric g^S . That it does not contain any \mathcal{M} -singular points is also confirmed by Fig 10A, which shows S (the green surface) together with R (red surface): they do not intersect. This changes for the symplectic leaf S' of Fig. 3: Fig 10B shows that S'

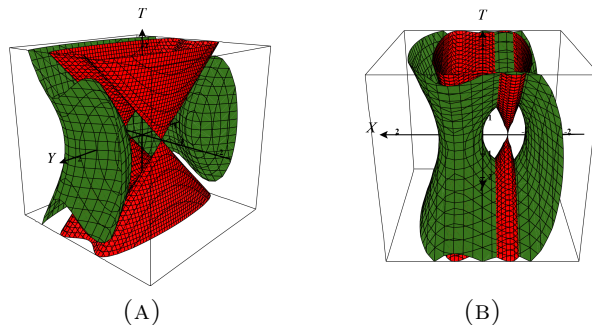


FIGURE 10. Intersecting the red zone R of $(\mathbb{R}^3, g, \Pi_{qua})$, drawn in red, with the two symplectic leaves, drawn in green, which are obtained for (A) $c = 1$ and (B) $c = 0$. While in (A) there are no intersections, in (B) there are (see also Fig. 10 below).

has non-empty intersections with R . Keeping only S' and the parts of R intersecting S' , we obtain Fig. 10. We call the admissible, i.e. \mathcal{M} -regular parts of a symplectic leaf of interest a **green zone** and each intersection of the leaf with the red zone a **red line**.⁵

In the class of examples discussed in this paper, there is a nice way of characterizing the red lines. Let us fix a symplectic leaf S_c corresponding to the value c of the Casimir function (4.4). Then we see that on the symplectic leaf S_c , we can express xy as a function of z only: $xy = \exp[-P(z)] \cdot [c - Q(z)]$. Plugging this into (6.7), we obtain a function $F_c = f|_{S_c}: \mathbb{R} \rightarrow \mathbb{R}$, which takes the form

$$F_c = U^2 + 2(1 + UV)e^{-P}(c - Q) + V^2 e^{-2P}(c - Q)^2. \quad (7.1)$$

It is precisely the zeros z_{red} of this function, $F_c(z_{red})$, that determine the red lines on the leaf S_c ; they consist of those points on S_c where the X -coordinate takes one of the values of the zeros of the function F_c ,

$$X \equiv z = z_{red}. \quad (7.2)$$

⁴More generally, one may want to call leaves S where \mathcal{M} -degenerate points form a subset of measure zero “almost good leaves”: there some care will be needed when approaching the forbidden red walls, but within a good region, the conditions for Theorem 3.4 to hold true are satisfied.

⁵The “red lines” might be called “red domain walls” for higher dimensional almost regular leaves.

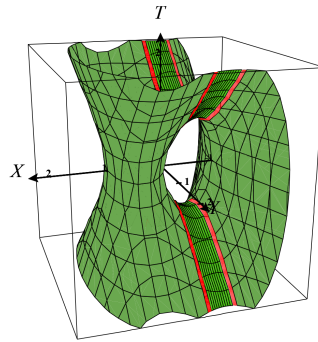


FIGURE 11. The green zones and red lines for the symplectic leaf corresponding to $c = 0$ in the example with quadratic brackets. The dark green region between the two red lines is of Euclidean signature, the light green regions left and right of the lines are of Lorentzian signature.

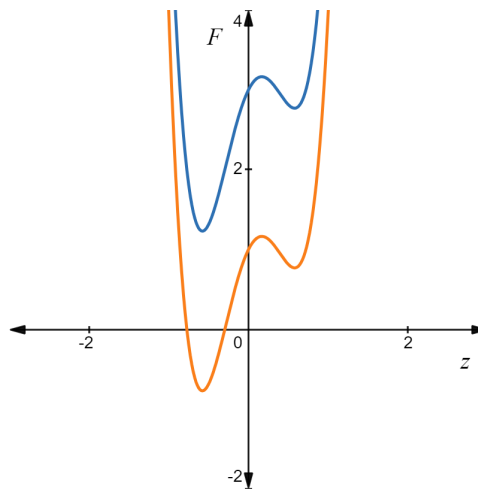


FIGURE 12. The function F_c for the quadratic Poisson structure, orange color for F_0 and blue color for F_1 .

It is remarkable that, for *every* choice of U and V , the intersection of the red zone with *any* symplectic leaf has a constant value for X .

Note that the intersection of the planes (7.2) with a symplectic leaf S gives the red lines only if $S = S_c$. Such as the zeros of the function h_c determine the topological nature of the (corresponding) symplectic leaf S_c of (M, Π) , the zeros of the function F_c determine the red lines and green zones of this leaf in (M, g, Π) . Moreover, if $F_c(z) > 0$, then for this value of z or X the induced metric has Lorentzian signature, and if $F_c(z) < 0$, it is Euclidean.

Let us return to the example of quadratic brackets for an illustration again: The function (7.1) becomes $F_c = 9z^4 - 2z^3 - 6z^2 + 2z + 1 + 2c$. Its graph is drawn in Fig. 12 for the two values of c corresponding to the leaves depicted in Fig. 2 ($c = 1$) and Fig. 3 ($c = 0$). We see from this diagram that for $c = 1$ there are no zeros of this function and that it

is strictly positive. This implies that the corresponding leaf S_0 , see Fig. 2, is a good leaf and that the induced metric is of Lorentzian signature everywhere. Certainly, we found this before already by other means, but we see that it can be deduced very easily from just the inspection of the graph of the one-argument function F_1 .

Likewise, we see that F_0 has two zeros. They are located at the values $z_{red,1} \approx -0.77$ and $z_{red,2} \approx -0.30$. This fixes the location of the two red lines on the leaf S_0 depicted in Fig. 11. Between these two values of $z \equiv X$ the function F_0 is negative and thus the region between the red lines, depicted as dark green in Fig. 11, is Riemannian. For values of X smaller than $z_{red,1}$ or bigger than $z_{red,2}$, F_0 is positive and therefore those green zones, depicted by light green in Fig. 11, carry an induced metric of Lorentzian signature.

8. GENERALIZED DOUBLE BRACKET VECTOR FIELD AS GRADIENT VECTOR FIELD IN GREEN ZONES

Now we turn to determining explicitly the geometric data on a regular symplectic leaf S , i.e. the induced metric g_{ind}^S and the symplectic form ω^S . The leaves result from imposing $C(x, y, z) = c$. Taking the differential of this equation, one has

$$x dy + y dx + W dz \approx 0. \quad (8.1)$$

Here and in what follows we use \approx for all equations valid on S only. Then, when using the coordinates (x, z) on S , one has

$$dy \approx -\frac{y dx + W dz}{x}. \quad (8.2)$$

We see that these coordinates cover regions of the leaf where $x \neq 0$. Likewise, when using (y, z) on the leaf, we get expressions valid for $y \neq 0$. Finally, the coordinates (x, y) are good coordinates on S whenever $W(x, y, z) \neq 0$. Since the simultaneous vanishing of x, y and W correspond precisely to the singular pointlike leaves, we see that we can cover all of S with these three coordinate charts. We will, henceforth, content ourselves with the coordinate chart (x, z) . For the other two charts one obtains similar expressions.

Plugging (8.2) into the embedding metric (6.1), we see that the induced metric becomes

$$g_{ind}^S \approx -\frac{2y}{x} dx^2 - \frac{2W}{x} dx dz + dz^2 \quad (8.3)$$

in the chart with $x \neq 0$. Here y is understood as the following function of x, z , and the parameter c :

$$y \approx \frac{e^{-P(z)} (c - Q(z))}{x} =: y(x, z), \quad (8.4)$$

where P and Q are the functions defined in Lemma 4.1. The coordinate y also enters W , so in (8.3)

$$W \approx U(z) + 2x y(x, z) V(z). \quad (8.5)$$

The apparent singularity of g_{ind}^S results from the fact that the coordinate system (x, z) on S breaks down for $x = 0$. We remark in parenthesis that this corresponds to the plane $Y = T$ in the coordinate system (4.7). On the other hand, there is an inherent problem

with g_{ind}^S when a point on the leaf S lies inside the red zone R , cf. (6.6): Calculating the determinant of the induced metric, we find

$$\det g_{\text{ind}}^S \approx -\frac{f^S(x, z)}{x^2}, \quad (8.6)$$

where $f^S(x, z) := f(x, y(x, z), z)$ with the function f as defined in (6.4). So, as expected, $\det g_{\text{ind}}^S$ vanishes on the red lines. This corresponds to

$$\ker \#_{g_{\text{ind}}^S} |_m \approx \text{Vect}(x\partial_x|_m + W\partial_z|_m) \quad \forall m \in R \cap S. \quad (8.7)$$

On the other hand, from the second Poisson bracket in (4.3), we deduce that

$$\omega^S \approx \frac{dx \wedge dz}{x}. \quad (8.8)$$

Certainly, ω^S is well-defined on all of the leaf S . The apparent singularity at $x = 0$ is a coordinate singularity.

This brings us to the position of determining the double-bracket metric (3.1). A direct calculation yields

$$\tau_{DB} \approx \frac{2ydx dx + 2W dx dz - x dz dz}{x(2xy + W^2)}, \quad (8.9)$$

with y and W as in (8.4) and (8.5) certainly. We remark that

$$\tau_{DB} \approx -\frac{1}{f^S} g_{\text{ind}}^S. \quad (8.10)$$

So evidently this tensor is not well-defined on the red lines, i.e. for the points $m \in R \cap S$ —and it also does not have a continuous continuation into such points. This is in contrast to g_{ind}^S , which is a well-defined tensor on all of S ; it just does not define a pseudo-metric on $R \cap S$, since there it has a kernel, see (8.7). In the green zones, however, i.e. on $S \setminus (R \cap S)$, both, g_{ind}^S and τ_{DB} , define a (pseudo) metric.

The second main ingredient in Theorem 3.4 is the generalized double bracket vector field $\partial_M G$, which is defined on all of $M = \mathbb{R}^3$ certainly. The easiest way to determine it for a function $G \in C^\infty(\mathbb{R}^3)$ at this point is—see (2.5)—to apply the *negative* of the matrix (6.2) to the vector $[dG] = (G_{,x}, G_{,y}, G_{,z})$, where the comma denotes the derivative with respect to the corresponding coordinate. This leads to

$$\begin{aligned} \partial_M G &= (-x^2 G_{,x} + [xy + W^2] G_{,y} - xW G_{,z}) \partial_x + \\ &\quad (-y^2 G_{,y} + [xy + W^2] G_{,x} - yW G_{,z}) \partial_y + \\ &\quad (-xW G_{,x} - yW G_{,y} + 2xy G_{,z}) \partial_z. \end{aligned} \quad (8.11)$$

To see how it arises from more geometrical quantities, we also display the three elementary Hamiltonian vector fields corresponding to the canonical coordinates $(x, y, z) \in \mathbb{R}^3$,

$$\begin{aligned} X_x &= W\partial_y - x\partial_z, \\ X_y &= -W\partial_x + y\partial_z, \\ X_z &= x\partial_x - y\partial_y. \end{aligned} \quad (8.12)$$

Now, \flat_g applied to any vector field $a\partial_x + b\partial_y + c\partial_z$ yields the 1-form $b dx + a dy + c dz$, and since $\sharp_\pi dx = X_x$ etc, we easily find the image of (8.12) under $\sharp_\pi \circ \flat_g$ to be

$$\begin{aligned}\sharp_\pi(\flat_g(X_x)) &= WX_x - xX_z, \\ \sharp_\pi(\flat_g(X_y)) &= -WX_y + yX_z, \\ \sharp_\pi(\flat_g(X_z)) &= xX_y - yX_x.\end{aligned}\tag{8.13}$$

Plugging (8.12) into (8.13), we obtain—cf. (2.6)—the three fundamental double bracket vector fields $\partial_{\mathcal{M}}x$, $\partial_{\mathcal{M}}y$, and $\partial_{\mathcal{M}}z$, respectively.

The vector field $\partial_{\mathcal{M}}G$ is defined on \mathbb{R}^3 , but it is tangent to the symplectic leaves and thus also to the singled-out leaf S . We thus can view the restriction $\partial_{\mathcal{M}}G|_S$ of $\partial_{\mathcal{M}}G$ to S as a vector field on S . To see what section in TS it is in our coordinate system (x, z) on S chosen above, we first express $\partial_{\mathcal{M}}G \in \Gamma(\mathbb{R}^3)$ in a coordinate system adapted to the symplectic leaves. We choose $\tilde{x} := x$, $\tilde{y} := C(x, y, z)$, and $\tilde{z} := z$; this is a good coordinate system on $\mathbb{R}^3 \setminus (\{0\} \times \mathbb{R}^2)$. Under such a coordinate change, ∂_x does not simply become $\partial_{\tilde{x}}$, for example, despite the fact that $x = \tilde{x}$, but one rather has

$$\partial_x = \partial_{\tilde{x}} + C_{,y} \partial_{\tilde{y}}.$$

However, since the vector field $\partial_{\mathcal{M}}G$ is tangent to the symplectic leaf S when restricted to it, all contributions proportional to $\partial_{\tilde{y}}$ will cancel out, while the ones proportional to ∂_x and ∂_z remain unchanged. Thus, in this new coordinate system, the vector field (8.11) takes the same form after replacing untilded coordinates by tilded ones and, at the same time, simply dropping the second line on the right-hand side.

Therefore, after the dust clears and using again the coordinates $x = \tilde{x}$ and $z = \tilde{z}$ as coordinates on the leaf S , we obtain

$$\partial_{\mathcal{M}}G|_S \approx (-x^2 G_{,x} + [xy + W^2] G_{,y} - xWG_{,z}) \partial_x + (-xWG_{,x} - yWG_{,y} + 2xyG_{,z}) \partial_z.\tag{8.14}$$

Here, the derivatives of G are taken before restricting to S , and, as before, the functions y and W are given by (8.4) and (8.5), respectively.

We are finally ready to combine the two main ingredients (8.9) and (8.14). After a somewhat tedious calculation and the cancellation of several terms, one obtains from this:

$$\tau_{DB}(\partial_{\mathcal{M}}G|_S, \cdot) \approx -G_{,x} dx + G_{,y} \left(\frac{y}{x} dx + \frac{W}{x} dz \right) - G_{,z} dz.\tag{8.15}$$

Upon usage of (8.2), the term in the brackets following $G_{,y}$ is recognized to be precisely $-dy$. This implies

$$\tau_{DB}(\partial_{\mathcal{M}}G|_S, \cdot) \approx -d(G|_S),\tag{8.16}$$

which is equivalent to Equation (3.2).

In the above manipulations, it is understood that one is within the green zone of S since otherwise τ_{DB} would not be defined (cf. (8.10) and the discussion following it). On the other hand, we see that according to the right-hand side of (8.16), the left-hand side has a continuous continuation to \mathcal{M} -singular points. This can be explained as follows: Recall that $\partial_{\mathcal{M}}G$ is a well-defined vector field on all of \mathbb{R}^3 and thus also the right-hand side of (8.14) is defined on $R \cap S$ if only $x \neq 0$ (applicability of our coordinate patch).

Using that on R we can replace $-2xy$ by W^2 , see (6.4) and (6.6), we find that in our chart (x, z) on S :

$$\partial_{\mathcal{M}}G|_{S \cap R} \approx (xG_{,x} + yG_{,y} + WG_{,z}) (x\partial_x + W\partial_z) . \quad (8.17)$$

On R , the image of $\sharp_{\mathcal{M}}$ becomes one-dimensional and, upon restriction to a leaf S coincides with the kernel of τ_{DB}^S there, see (8.7). So, while τ_{DB} simply blows up on R , see (8.10), it is not simply that the vector field $\partial_{\mathcal{M}}G$ would go to zero there to compensate for the singularity in τ_{DB} . Instead, approaching a point m in the red zone, it more and more turns into the direction of the non-zero kernel of $f^S \tau_{DB}$ at such an m .

Conclusions. In this paper we have generalized the double vector field construction defined originally only on semi-simple Lie algebras to general pseudo-Riemannian Poisson manifolds. The generalized double bracket vector field has some useful properties. It is tangent to all the symplectic leaves. Moreover, when restricted to such a leaf, it proves to be of gradient type. This happens with respect to a metric on the leaf which generalizes the normal metric on adjoint orbits in compact semi-simple Lie algebras.

In the case of a Poisson manifold with metric of indefinite signature, the generalization works only on regions where the metric induced on the symplectic leaves is non-degenerate. These regions are called green zones and leaves for which the induced metric is non-degenerate everywhere are called good leaves. We have provided a characterization of such regions which avoids determining the induced metric explicitly, which can become quite complicated. All this have been illustrated for a wide class of Poisson structures on \mathbb{R}^3 , which we have discussed in full detail.

Acknowledgements. Z. Ravanpak acknowledges a scholarship ‘‘Cercetare postdoctorală avansată’’ funded by the West University of Timișoara, Romania, and the financial support from the Spanish Ministry of Science and Innovation under grants PID2022-137909NB-C22. The authors are grateful to Thomas Strobl for valuable discussions and helpful suggestions to improve significantly the presentation of the paper.

REFERENCES

- [1] P.A. Absil, R. Mahony, R. Sepulchre, *Optimization Algorithms on Matrix Manifolds*, Princeton University Press, 2008.
- [2] M. F. Atiyah, *Convexity and commuting Hamiltonians*, Bull. London Math. Soc., vol. **14**, 1-15 (1982).
- [3] A. Ballesteros, J. C. Marrero and Z. Ravanpak, *Poisson-Lie groups, bi-Hamiltonian systems and integrable deformations*, *J. Phys. A Math. Theor.* **50**, 145204 (2017).
- [4] A. L. Besse, *Einstein manifolds*, Springer-Verlag, Berlin, 1987.
- [5] P. Birtea, D. Comănescu, *Geometric dissipation for dynamical systems.*, Comm. Math. Phys. 316, 375-394 (2012).
- [6] P. Birtea, D. Comănescu, *Hessian operators on constraint manifolds*, J. Nonlinear Science 25, 1285-1305 (2015).
- [7] P. Birtea, D. Comănescu, *Asymptotic Stability of Dissipated Hamilton-Poisson Systems*, SIAM Journal on Applied Dynamical Systems 8 (3), 967-976 (2009).
- [8] A.M. Bloch, *Steepest descent, linear programming and Hamiltonian flows*, Contemp. Math. AMS, vol. **114**, 77-88 (1990).
- [9] A.M. Bloch, R.W. Brockett, T.S. Ratiu, *Completely integrable gradient flows*, Commun. Math. Phys., vol. **147**, 57-74 (1992).

- [10] A.M. Bloch, H. Flaschka, T.S. Ratiu, *A convexity theorem for isospectral sets of Jacobi matrices in a compact Lie algebra*, Duke Math. J., vol. **61**, 41-66 (1990).
- [11] R.W. Brockett, *Dynamical systems that sort lists, diagonalize matrices, and solve linear programming problems*, Linear Algebra Appl., vol. **146**, 79-91 (1991).
- [12] R.W. Brockett, *Differential geometry and the design of gradient algorithms*, Proc. Symp. Pure Math., vol. **54** (I), 69-92 (1993).
- [13] A. Edelman, T. A. Arias, S. T. Smith, *The geometry of algorithms with orthogonality constraints*, SIAM J. Matrix Anal. Appl., Vol. **20**, Issue 2, 303-353 (1998).
- [14] I. Gutierrez-Sagredo, D. Iglesias Ponte, J. C. Marrero, E. Padrón, Z. Ravanpak, *Unimodularity and invariant volume forms for Hamiltonian dynamics on Poisson-Lie groups*, J. Phys. A: Math. Theor. **56** 015203, (2023).
- [15] T. Klösch and T. Strobl, *Classical and quantum gravity in dimensions: I. A unifying approach*, Class.Quant.Grav. **13** (1996) 965-984; Erratum-ibid. **14** (1997) 825.
- [16] P.J. Morrison, *Bracket formulation for irreversible classical fields*. Phys. Lett. A 100, 423-427 (1984).
- [17] P.J. Morrison, *A paradigm for joined Hamiltonian and dissipative systems*. Physica D 18, 410-419 (1986).
- [18] P.J. Morrison, M.H. Updike, *Inclusive curvaturelike framework for describing dissipation: Metriplectic 4-bracket dynamics*, Phys. Rev. E 109, 045202 (2024).
- [19] B. O'Neill, *Semi-Riemannian geometry with applications to relativity*, 1st Edition, Volume **103**, 1983.
- [20] I. Vaisman, *Lectures on the geometry of Poisson manifolds*, Progress in Mathematics, vol. **118**, Birkhäuser Verlag, Basel, 1994.

P. BIRTEA: DEPARTMENT OF MATHEMATICS, WEST UNIVERSITY OF TIMIȘOARA,
Email address: `petre.birtea@e-uvt.ro`

Z. RAVANPAK: DEPARTMENT OF MATHEMATICS, WEST UNIVERSITY OF TIMIȘOARA,
Email address: `zohreh.ravanpak@e-uvt.ro`

C. VIZMAN: DEPARTMENT OF MATHEMATICS, WEST UNIVERSITY OF TIMIȘOARA,
Email address: `cornelia.vizman@e-uvt.ro`